Investigation of hot and chemically reacting supersonic and subsonic flows using Laser-induced Thermal Acoustics

Annika Hell[⋆] *and Bernhard Weigand*[⋆]
[⋆]*Institut für Thermodynamik der Luft- und Raumfahrt (ITLR), Universität Stuttgart*
ITLR, Pfaffenwaldring 31, 70569 Stuttgart, Germany

Abstract

Experimental data bases are necessary for CFD code validation. Data acquisition is especially for supersonic combustion a challenging task. In future we will probe supersonic chemically reacting free jets as basic validation case using the seedless nonintrusive technique Laser-induced Thermal Acoustics (LITA). To prove the reliability of LITA, test cases are necessary. Here we present LITA measurements in premixed laminar methane/air flames produced by a McKenna burner. The comparison with coherent anti-Stokes Raman spectroscopy (CARS) measurements showed a maximum deviation that is within the measurement accuracy of 2.2 %. Furthermore LITA measurements within a turbulent supersonic air/air free jet at a total temperature of $T_t \approx 1300$ K are presented and compared to CFD predictions. Good agreement between experimental data and numerical simulations is found.

1. Introduction

The airbreathing scramjet engine is a promising propulsion concept for future space transportation systems and also for hypersonic civil transport aircrafts. Worldwide, great effort is put into the development of scramjet engines. Also the research training group GRK 1095/2 'Aero-Thermodynamic Design of a Scramjet Propulsion System for Future Space Transportation Systems' is working on the design and development of a scramjet demonstrator. The main part of the scramjet engine is the combustion chamber. Especially the understanding of supersonic combustion is essential. As none of the current ground test facilities is capable of perfectly reproducing the flight conditions of a real engine, computational fluid dynamics (CFD) codes, which are used to analyze high speed flows, fuel-air mixing, and combustion, are important tools for development and design verification processes. Nevertheless, experimental databases are necessary for CFD code validation.

Axisymmetric, coaxial, chemically reacting free jets serve as basic validation cases for supersonic combustion since they provide good optical access and taking advantage of the symmetry the number of spatial measurement points can be minimized. Since conventional probe techniques are limited to cold, non reacting flows, non intrusive measurement techniques have to be used. The established laser based techniques for scramjet combustor research are particle image velocimetry (PIV) [1] and coherent anti-Stokes Raman spectroscopy (CARS) [2, 3]. These measurement techniques have some disadvantages. The main disadvantage of PIV is the need of seeding particles. The use of CARS is expensive and the technique is sensitive to environmental conditions. Cutler et al. performed CARS and interferometric Rayleigh scattering (IRS) simultaneously to probe chemically reacting coaxial axisymmetric free jets. They measured temperature, species mole fraction, and velocity profiles in a laboratory scale burner with a nozzle exit diameter of $d = 10$ mm successfully [4, 5]. Afterwards they performed measurements in a large scale setup (nozzle exit diameter $d = 63.5$ mm) at NASA Langley's Direct Connect Supersonic Combustion Test Facility. The description of the facility and a preliminary analysis of the measurements can be found in [6] and [7], respectively. Due to harsh environmental conditions at the test facility and associated perturbations like beam steering only temperature and velocity measurements in a $Ma = 5.5$ combustion-heated air jet with a total temperature of $T_t = 1327$ K (nominal condition) are presented and analyzed in [8] and [9].

In future we will investigate a $Ma = 1.45$ chemically reacting H_2/Air free jet using the Laser-induced Thermal Acoustics (LITA) measurement technique. With LITA speed of sound is measured directly and with a modification velocity measurements are also possible. The advantages of LITA are the simple setup (compared to CARS) and robustness against environmental conditions. So far we investigated unheated ($T_t = 292$ K) and heated ($T_t = 550$ K) subsonic and supersonic air free jets as validation cases for LITA. The comparison of LITA to conventional probe measurements (wall pressure distribution, Pitot pressure, total temperature) and CFD predictions showed a very good agreement [10]. Furthermore we investigated mixing free jets of air/air, He/air and CO_2/air at temperatures up to $T_t = 620$ K. The results showed also a very good agreement with probe measurements and CFD predictions [11]. In this paper we present the results of an additional validation case to prove the reliability of LITA measurements in chemically reacting flows. For that purpose we investigated different methan/air flames produced with a McKenna flat flame burner and compared the results with CARS measurements [12]. Furthermore, preliminary results of speed of sound measurements in a hot ($T_t \approx 1300$ K) air/air free jet are presented.

2. Experimental Setup

2.1 Laboratory McKenna Burner

To prove the reliability of LITA measurements in flames, we investigated different premixed, laminar methan/air flames produced with a commercially available flat flame burner (Holthuis & Associates formerly McKenna). The burner is made of stainless steel. The outer diameter is 120 mm and the height is 60 mm. The burner matrix is made of sintered bronze in which a cooling circuit is sintered. The matrix diameter is 60 mm. It is surrounded by a shroud ring that can be used to generate an annular coflow. This possibility was not used in these experiments. Cooling water flow was regulated by a rotameter and set to 1 l/min. Air and methane flow were regulated by digital massflowmeters (Bronkhorst, EL-FLOW). The maximum flow for air and methane is 35 slpm (slpm: standard liter (273 K, 1013 hPa)and 5 slpm, respectively. The uncertainty is less than 1 %. Purity of the used methane is 99.5 %. We wanted to compare our measurements with CARS measurements [12]. Therefore, measurements were located 15 mm above the burner plate. This point was chosen because of the good optical access and negligible temperature gradients at this height. Three different burner of the same kind were compared [12]. The comparison showed a discrepancy of less than 3 % for the measured temperatures. Therefore, they are within the measurement uncertainty of CARS measurements (3 – 4 %). Thus, the error due to different burners is within measurement uncertainty and thus negligible.

2.2 Supersonic Combustion Test Facility

At the Institut für Thermodynamik der Luft- und Raumfahrt (ITLR) free jets are generated using the continuously operating supersonic combustion facility (see Figure 1). It is described in more detail by Kasal et al. [13]. Briefly, it consists of a 500 kW screw compressor fed by atmospheric air. After compression the air is dried in a dehumidifier. Then the air can be heated by a two-stage electric heater with a total power consumption of 1 MW.

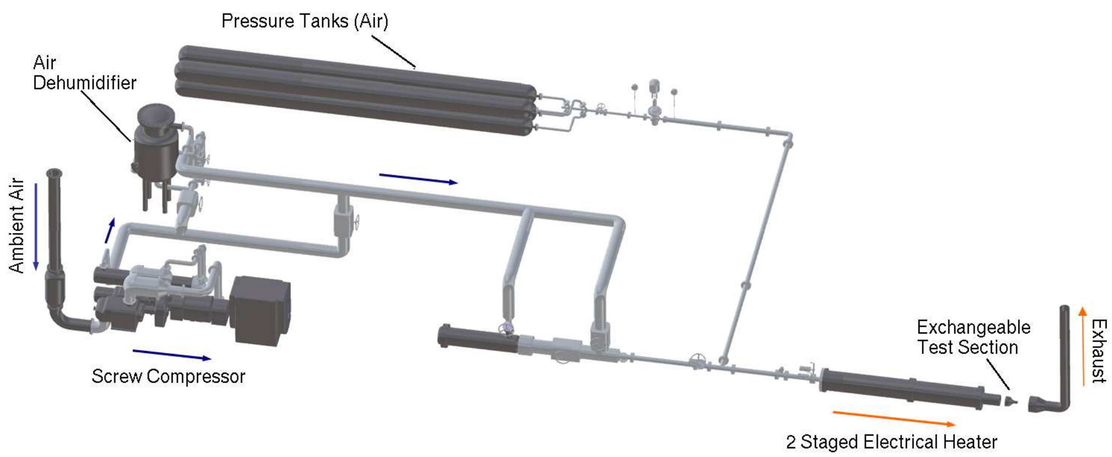

Figure 1: Supersonic combustion test facility at the ITLR

The facility delivers an air flow with a maximum total temperature of $T_t = 1500\,\mathrm{K}$ and a maximum mass flow of $\dot{m} = 1.45\,\mathrm{kg/s}$ at a maximum total pressure of $p_t = 10\,\mathrm{bar}$. The heated air is fed into one of a selection of test sections, e.g. combustion chamber, film cooling channel, and nozzles for free jet generation. The used nozzle in these experiments is shown in Figure 2. A detailed mechanical drawing of the nozzle is attached (Figure 11).

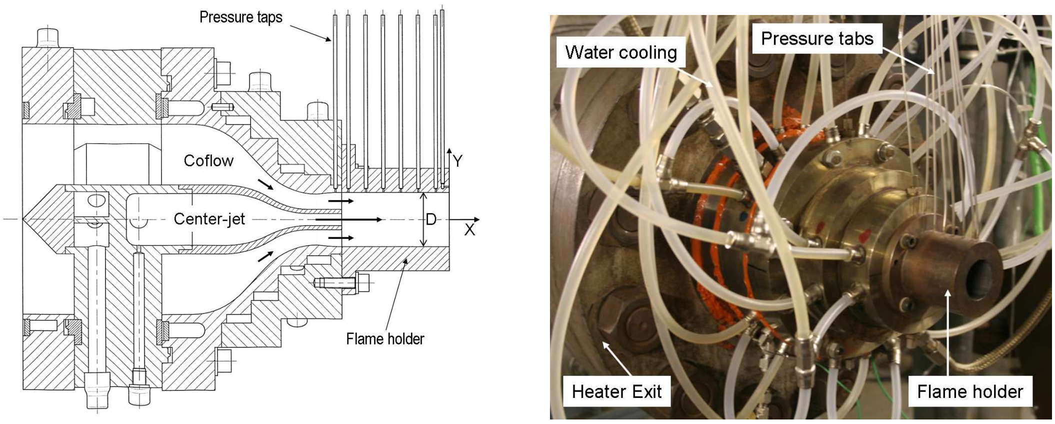

(a) Cross sectional view of the supersonic nozzle

(b) Image of the nozzle installed in the supersonic combustion facility at ITLR

Figure 2: Supersonic nozzle

It is a stainless steel, water cooled, coaxial nozzle. The air flow is accelerated in the convergent-divergent outer part of the nozzle to an exit Mach number of $Ma = 1.45$. Test gases or fuel are injected at sonic speed into the air flow through the inner convergent nozzle. In the subsonic part of both nozzles pressure holes for static wall pressure measurements exist and thermocouples can be installed. We used type K thermocouples (Omega, OMEGACLAD XL) to measure total temperatures at the nozzle entrance. The flame holder increases the mixing efficiency and the flame stability in case of a chemically reacting free jet. It contains seven pressure taps for static wall pressure measurements.

2.3 Measurement Technique

Due to the limited use of conventional intrusive probe measurements to cold, non reactive flows, the nonintrusive, seedless, laser based technique Laser-induced Thermal Acoustics (LITA) is used to investigate highly turbulent, supersonic flows at high temperatures. LITA measures the local speed of sound in a test volume directly [14, 15]. With a modified setup flow velocity [16, 17] and gas composition [18, 19] can be measured. In a previous work at the ITLR we proved the reliability of LITA measurements in turbulent, supersonic mixing flows with temperatures up to $T_t = 620\,\mathrm{K}$ [10, 11]. The optical setup is shown in Figure 3.

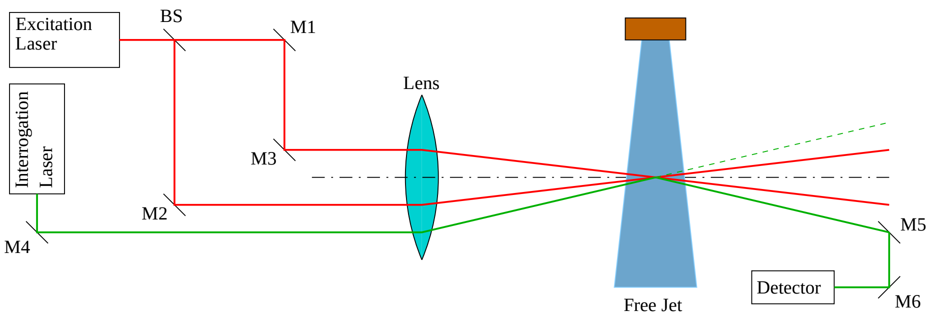

Figure 3: Optical LITA Setup

For LITA two laser beams are necessary. One beam is the so called excitation beam (red, wavelength $\lambda_{exc} = 1064\,\mathrm{nm}$). It is split by a 50 % beam splitter (BS) into two parts. The beams are parallel aligned by a mirror system (M) and focused by a lens. The beam intersection area defines the size of the test volume. In our case it has a length of $l \approx 7.4$ mm and a diameter of $d \approx 0.18$ mm. In place of the intersection, an interference grating is formed. The electric field distribution, corresponding to the interference grating, influences the test medium so that a density grating is formed. The driving phenomena of the density grating formation are electrostriction and thermalization. The term electrostriction denotes the polarization and acceleration of molecules due to an electric field. The term thermalization denotes density modifications due to thermal heating. The other beam is the so called interrogation beam (green, wavelength $\lambda_{int} = 532$ nm). It detects the temporal evolution of the density grating. It is focused by the same lens as the excitation beam. The small part of the interrogation beam that is reflected on the density grating is the signal beam. The detected signal has the shape of a damped oscillation. The oscillation is damped due to dissipative effects such as thermal dissipation. The signal frequency is proportional to the speed of sound. The setup is described in more detail in [11].

3. Numerical Setup

In addition to the experiments, numerical simulations of the nozzle flow and the supersonic mixing free jets were performed. The calculations were done by the commercial, finite-volume CFD code FLUENT™ 12.1, assuming an axisymmetric flow of perfect gases. The calculations are carried out assuming steady state and compressible flow. Turbulence is modeled via a Standard k-ϵ model. The diffusion terms in the discretized scalar transport equation are central-differenced and second-order accurate. Convection terms are calculated using the second-order upwind Roe flux-difference splitting scheme.

Structured grids are used for the calculation and are generated by the commercial code GAMBIT™. Near the nozzle walls the grid points are clustered to resolve the boundary layer and in the vicinity of the center-jet nozzle to resolve recirculation zones and shocks (Figure 4). The dimensionless distance between wall and first cell center

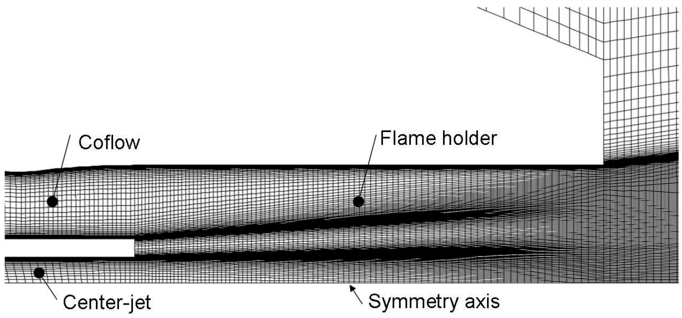

Figure 4: Mesh of the supersonic flow at nozzle exit

is less than $y_1^+ = 1$. The grid consists of 146,006 cells. In the course of a grid convergence study, simulations on a finer (290,580 cells) and a coarser (72,940 cells) grid were performed. The obtained results showed no significant difference. In the run-up to the simulations similar nozzle flows were investigated. A comparison of experimental data and numerical simulation of this validation cases resulted in an uncertainty of 3%. The uncertainties of the simulations of the mixing free jet are assumed to be in the same range and thus comparable to the uncertainties for speed of sound measurements.

4. Results

4.1 Laboratory McKenna Burner

We investigated 21 different methan/air flames. The characteristic data of the flames are summarized in Table 1. Here $\dot{m}$ gives the air and methane mass flows, Φ is the resulting equivalence ratio, T_{ad} and T_{CARS} are the adiabatic flame temperature and the temperature measured with CARS [12], respectively. The discrepancy between adiabatic and measured temperature is due to heat losses to the water cooled burner surface. Taking the measured temperature and assuming chemical equilibrium, gas composition and speed of sound are calculated using the chemical equilibrium solver 'Gaseq' [12]. The variables X(species) give the mole fraction of the main species, a_{Gaseq} and a_{LITA} are calculated and measured speed of sound values, respectively.

Table 1: Characteristic data of 21 different methan/air flames for the McKenna burner

Nr.	$\dot{m}_{CH_4}$ slpm/min	$\dot{m}_{Air}$ slpm/min	Φ	T_{ad} K	T_{CARS} K	$X(0_2)$	$X(N_2)$	$X(H_2O)$	$X(C0_2)$	$X(CO)$	$X(H_2)$	a_{Gaseq} m/s	a_{LITA} m/s
1	1.100	15.00	0.70	1838	1706	0.0578	0.7350	0.1367	0.0684	0.0000	0.0000	802.7	815.16
2	1.310	15.60	0.80	1997	1765	0.0379	0.7279	0.1547	0.0774	0.0001	0.0000	816.4	812.88
3	1.310	12.40	1.00	2226	1790	0.0005	0.7144	0.1894	0.0942	0.0008	0.0004	823.2	833.62
4	1.310	11.31	1.10	2211	1754	0.0000	0.6951	0.1886	0.0793	0.0223	0.0147	825.3	818.73
5	1.310	10.40	1.20	2137	1723	0.0000	0.6764	0.1844	0.0673	0.0406	0.0313	828.3	832.5
6	1.420	15.00	0.90	2134	1799	0.0185	0.7209	0.1723	0.0862	0.0001	0.0001	824.5	829.32
7	1.733	20.63	0.80	1997	1828	0.0376	0.7276	0.1546	0.0774	0.0001	0.0001	830.3	835.98
8	1.733	16.50	1.00	226	1886	0.0009	0.7138	0.1888	0.0933	0.0016	0.0008	844.5	841.32
9	1.733	14.96	1.10	2211	1826	0.0000	0.6951	0.1891	0.0788	0.0229	0.0141	841.4	838.23
11	1.733	13.70	1.20	2137	1828	0.0000	0.6763	0.1857	0.0660	0.0419	0.0300	852.2	841.89
12	1.733	11.80	1.40	1980	1813	0.0000	0.6417	0.1731	0.0486	0.0708	0.0656	868.7	861.38
13	2.050	15.00	1.30	2057	1878	0.0000	0.6585	0.1809	0.0554	0.0584	0.0466	873.5	873.5
14	2.287	15.00	1.45	1942	1915	0.0000	0.6336	0.1711	0.0435	0.0786	0.0729	896.8	887.4
15	2.550	30.30	0.80	1997	1967	0.0371	0.7268	0.1540	0.0770	0.0004	0.0002	860.4	859.1
16	2.550	27.00	0.90	2134	1976	0.0182	0.7201	0.1716	0.0856	0.0007	0.0003	862.9	861.08
17	2.550	24.14	1.00	2226	2009	0.0017	0.7128	0.1877	0.0917	0.0031	0.0014	871.4	875.46
18	2.550	22.00	1.10	2211	1934	0.0000	0.6950	0.1897	0.0780	0.0237	0.0134	865.1	865.04
19	2.550	20.20	1.20	2137	1883	0.0000	0.6763	0.1863	0.0653	0.0426	0.0293	864.5	859.6
20	2.550	17.43	1.39	1980	1929	0.0000	0.6433	0.1757	0.0474	0.0715	0.0618	894	881.6
21	3.420	32.40	1.00	2226	2100	0.0029	0.7111	0.1860	0.0891	0.0055	0.0023	891.1	891.05

For a better comparison the results are plotted in Figure 5. The uncertainty of CARS measurements is specified as 3 – 4 % [12]. We determined the uncertainty of the presented LITA measurements to 2.2 %. The maximum deviation between the calculated (CARS) and measured (LITA) speed of sound values is 1.5 % thus within measurement uncertainty. To sum it up, we have an excellent agreement between CARS and LITA measurements and therefore proved the reliability of our LITA setup for chemically reacting flows.

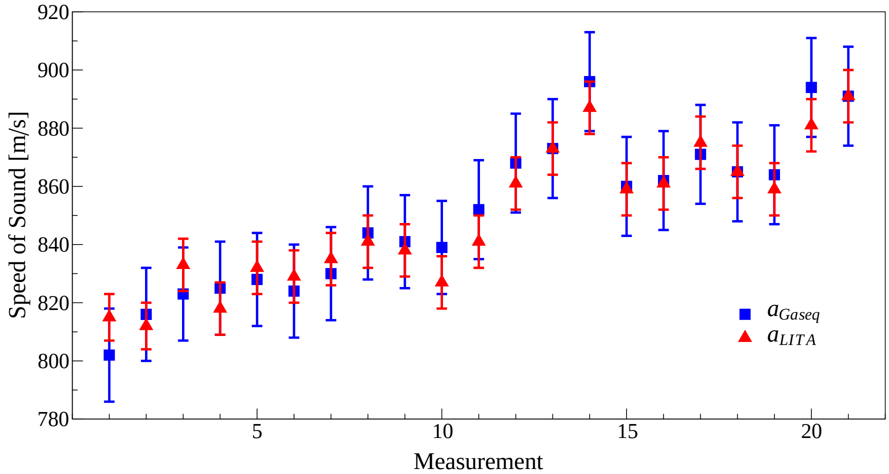

Figure 5: Comparison of LITA and CARS measurements in 21 different methane/air flames for the McKenna burner

4.2 Supersonic Free Jet

As another validation case for the LITA setup we investigated a turbulent supersonic free jet at a total temperature of $T_t = 1300\,\mathrm{K}$. To measure at different positions within the free jet, the LITA setup was mounted on a computer controlled three-axis translation table. The flow parameters for the experiment are summarized in Table 2. With the same boundary conditions a numerical simulation was performed.

Table 2: Experimental flow parameters for the supersoinic free jet experiment

	coflow	**center-jet**	**environment**
p_t [bar]	3.32	1.57	0.96
T_t [K]	1300	360	290

In Figure 6 shock and expansion structures are visualized by numerical schlieren, which are formed in the flame holder. The white lines are isolines for $Ma = 1$. Note that the center jet leaves the nozzle with $Ma = 1$. Due to the shock and expansion structure the flow is decelerated and accelerated again. The dashed lines indicate the investigated planes X/D, which are located downstream the flame holder exit at multiples of the nozzle exit diameter $D = 31.4$ mm. The dot-dashed lines mark the positions 1-7 of the pressure measurement.

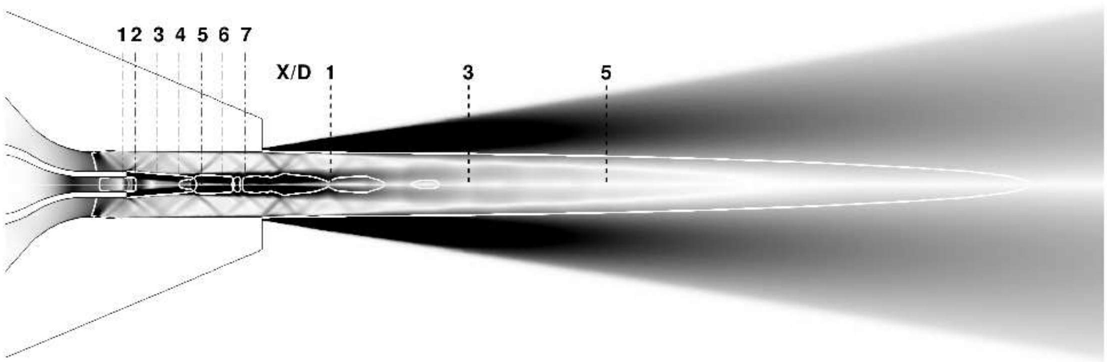

Figure 6: Numerical schlieren picture of the supersonic air/air free jet

Measured and numerically predicted static wall pressure distribution in the coflow nozzle and the flame holder are plotted in Figure 7. The dashed line indicates the transition from coflow nozzle to flame holder. The pressure rise at the flame holder exit is due to overexpansion and adjusts the pressure to ambient pressure. Except the last shock structure in front of the flame holder exit (position 6), which is predicted a bit too far upstream, numerical prediction and experiments show a very good agreement.

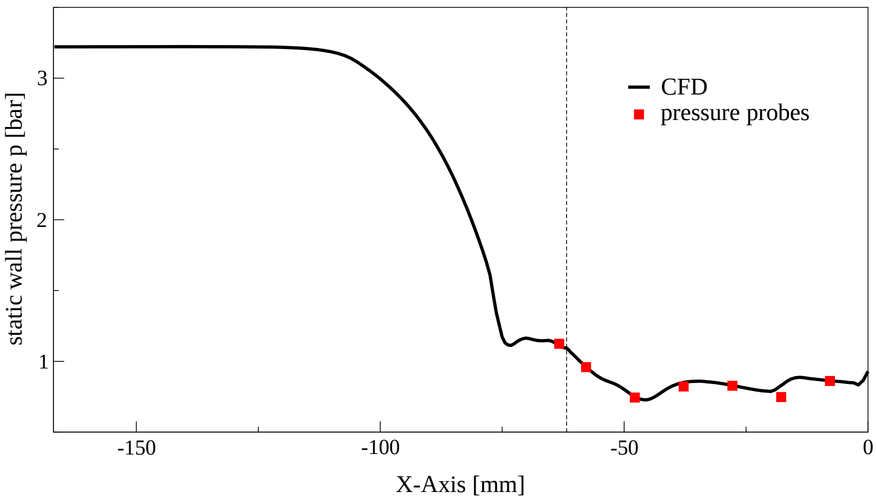

Figure 7: Static wall pressure distribution in the supersonic nozzle

The results of the LITA measurements in the planes X/D = 1, 3 and 5 within the free jet are plotted in Figure 8. Using the axisymmetry of the free jet only half of the plane was probed. The results are mirrored at the X axis for a better demonstration. The spreading of the free jet and the mixing layer growth are visible.

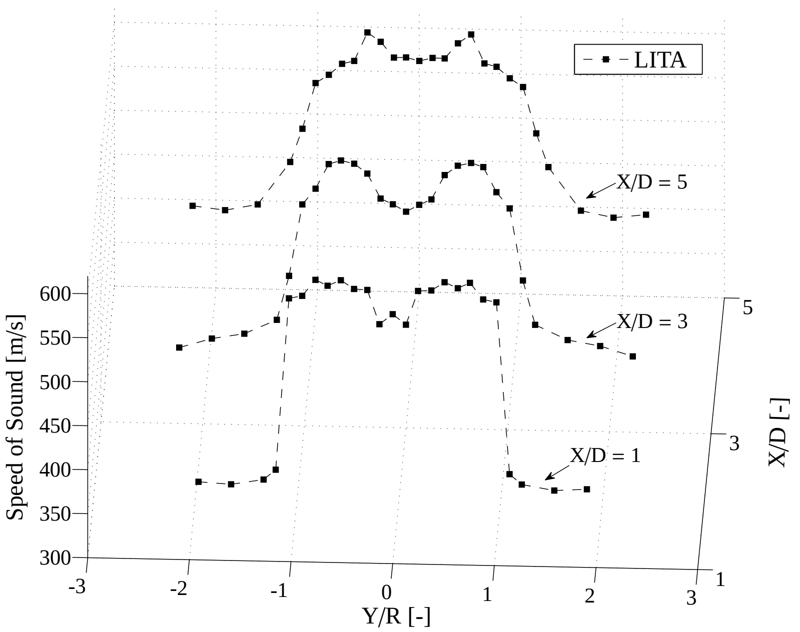

Figure 8: Measured speed of sound distribution for three planes within the supersonic air/air free jet

In plane 1, there is an unexpected increase of the speed of sound value at the X axis. That may be explained by the fact that the nozzle is not operated at matched conditions and a shock and expansion structure is formed within the free jet. These structures have an influence on the speed of sound distribution at the X axis as one can see in Figure 9. There the numerically simulated speed of sound and the measured values on the X axis are shown. The dashed line indicates the flame holder exit. In plane X/D = 1 the simulation predicts an incident shock on the axis, which can not be observed in the measurement.

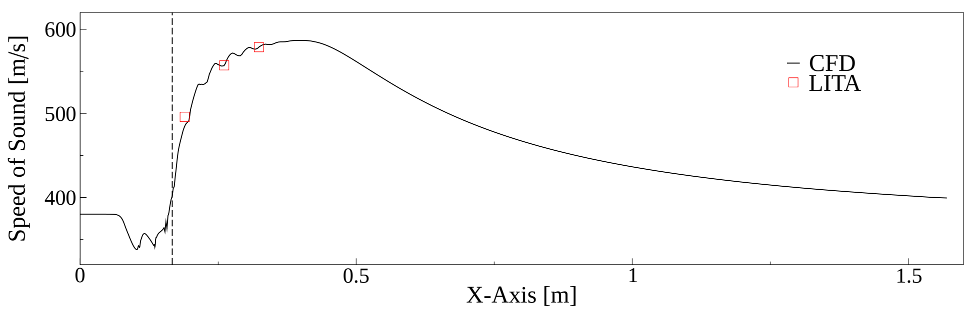

Figure 9: Predicted and measured speed of sound distribution along the X-Axis

In Figure 10 radial profiles of the LITA measurements (triangles) and numerical predictions (line) are plotted for the three investigated planes. Taking into account that the measurement volume of the LITA setup has a length of $l \approx 7.4\,\mathrm{mm}$, an average value of the numerically predicted speed of sound values was calculated (circles). The comparison shows that the maximum deviation (around 8 %) occurs in the shear layers between coflow and environment and coflow and center jet where steep gradients can be observed. The highest deviation (around 12 %) occurs at the center jet area in plane X/D = 1. As mentioned earlier, this may be explained by shock and expansion structures that are not predicted correctly.

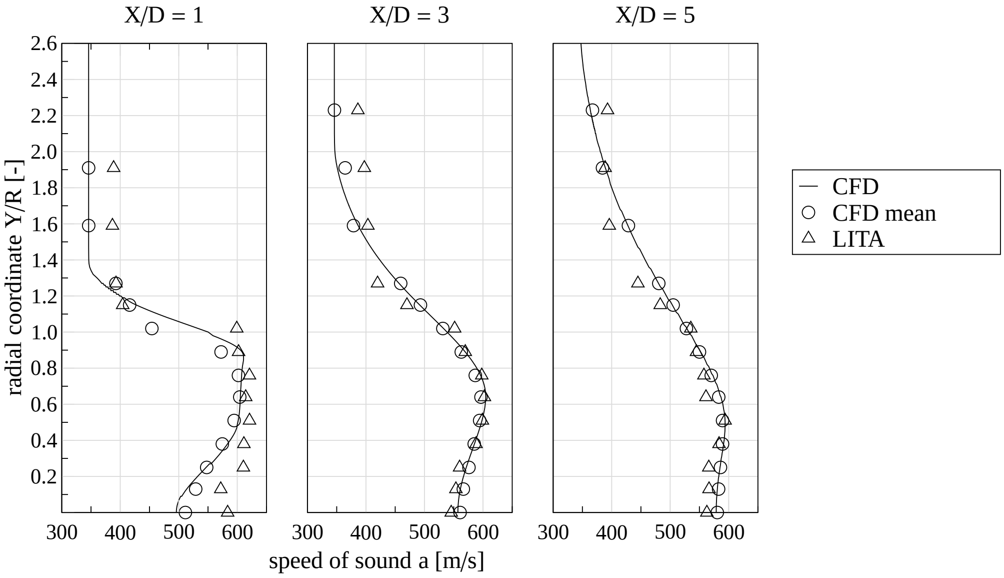

Figure 10: Measured and numerically predicted speed of sound distribution in three planes within the supersonic air/air free jet

5. Conclusion

To prove the reliability of LITA measurements in chemically reacting flows, premixed laminar methane/air flames produced with a McKenna flat flame burner were investigated. The results were compared to CARS measurements [12]. The maximum deviation is 1.5 % and thus within the LITA measurement uncertainty of 2.2 %. Therewith we proved the reliability of our LITA setup for chemically reacting flows.

Furthermore, a turbulent, supersonic, coaxial, axisymmetric free jet at a temperature of $T_t = 1300$ K was investigated. It was generated in the supersonic combustion test facility at the ITLR. The presented data are preliminary results. For a detailed analysis further data are necessary. We found a very good agreement between numerical simulation and static wall pressure measurements within the nozzle. Three planes perpendicular to the X axis are probed by LITA. The planes are located downstream the nozzle exit at 1, 3, and 5 times the nozzle exit diameter $D = 31.4$ mm. Maximum deviation of 12 % between numerical simulation and LITA occurs in plane 1 and in the shear layers between environment, coflow, and center jet. With increasing distance to the nozzle exit, the agreement between LITA and numerical simulation increases.

Acknowledgments

This work was performed within the Research Training Group 'Aero Thermodynamic Design of a Scramjet Propulsion System for Future Space Transport Vehicles' (GRK 1095). The authors would like to thank the German Research Foundation (Deutsche Forschungsgemeinschaft) for its financial support of this work.

References

[1] Goyne, C.P., McDaniel, J.C., Krauss, R.H., Day, S.W. *Velocity Measurement in a Dual-mode Supersonic Combustor using Particle Image Velocimetry*, AIAA Paper 2001-1761, 10th AIAA/NAL-NASDA-ISAS International Space Planes and Hypersonic Systems and Technologies Conference, Kyoto, Japan, 2001.

[2] Weisgerber, H., Fischer, M., Magens, E., Beversdorff, M., Link, T., Koschel, W. *Experimental and Numerical Analysis of an Expansion Flow in Chemical and Thermal Nonequilibrium*, 14th International Society for Air Breathing Engines- ISOABE, ISABE- International Symposium on Air Breathing Engines, Florence, Italy, 1999.

[3] Cutler, A.D., Danehy, P.M., Springer, R.R., O'Byrne, S., Capriotti, D.P., DeLoach, R. Coherent Anti-Stokes Raman Spectroscopic Thermometry in a Supersonic Combustor, *AIAA Journal* 41 (2003), No.12, pp.2451-2459.

[4] Cutler, A.D., Magnotti, G., Baurle, R., Bivolaru, D., Tedder, S., Danehy, P.M., Weikl, M.C., Beyrau, F., Seeger, T. *Development of Supersonic Combustion Experiments for CFD Modeling*, AIAA-2007-978, 45th AIAA Aerospace Sciences Meeting and Exhibit, Reno, Nevada, 2007.

[5] Tedder, S., Bivolaru, D., Danehy, P.M., Weikl, M.C., Beyrau, F., Seeger, T., Cutler, A.D. *Characterization of a Combined CARS and Interferometric Rayleigh Scattering System*, AIAA-2007-871, 45th AIAA Aerospace Sciences Meeting and Exhibit, Reno, Nevada, 2007.

[6] Cutler, A.D., Magnotti, G., Capriotti, D.P., Mills, C.T. *Supersonic Combusting Jet Experiments for Code Development and Validation*, 55th JANNAF/42nd combustion/30th Airbreathing Propulsion/30th Exhaust Plume Technology/24th Propulsion Systems Hazards/12th SPIRITS User Group Joint Subcommittee Meeting, Newton, MA, 2008.

[7] Danehy, P.M., Magnotti, G., Bivolaru, D., Tedder, S., Cutler, A.D. *Simultaneous Temperature and Velocity Measurements in a Large-Scale Supersonic, Heated Jet*, 55th JANNAF/42nd combustion/30th Airbreathing Propulsion/30th Exhaust Plume Technology/24th Propulsion Systems Hazards/12th SPIRITS User Group Joint Subcommittee Meeting, Newton, MA, 2008.

[8] Tedder, S., Danehy, P.M., Magnotti, G., Cutler, A.D. *CARS Temperature Measurements in a Combustion-Heated Supersonic Jet*, AIAA 2009-524, 47th AIAA Aerospace Sciences Meeting Including The New Horizons Forum and Aerospace Exposition, Orlando, Florida, 2009.

[9] Bivolaru, D., Cutler, A.D., Danehy, P.M., Gaffney, Jr R.L., Baurle, R.A. *Spatially and Temporally Resolved Measurements of Velocity in a* H_2*-air Combustion-heated Supersonic Jet*, AIAA 2009-0027, 47th AIAA Aerospace Sciences Meeting Including The New Horizons Forum and Aerospace Exposition, Orlando, Florida, 2009.

[10] A. Hell, E. Rosenko, B. Weigand, S. Schlamp: *Study of subsonic and supersonic free jets*. 3rd European Conference for Aerospace Science (EUCASS), Versailles, July 2009.

[11] A. Hell, E. Rosenko, B. Weigand, S. Schlamp: *Experimental and Numerical Study of Axisymmetric Supersonic Mixing Free Jets*. AIAA-2009-7406, 16th AIAA/DLR/DGLR International Space Planes and Hypersonic Systems and Technology Conference, Bremen, 2009.

[12] P. Weigand, R. Lückerath, W. Meier: *Documentation of a Flat Premixed Laminar* CH_4*/Air Standard Flames Temperatures and Species Concentrations*. available at `http://www.dlr.de/vt/desktopdefault.aspx/tabid-3065/4632_read-6696/` (accessed: 23.09.2010).

[13] Kasal, P., Gerlinger, P., Walther, R., von Wolfersdorf, J., Weigand, B.: *Supersonic Combustion: Fundamental Investigations of Aerothermodynamic Key Problems*, AIAA-2002-5119, 11th AIAA/AAAF International Conference, Orleans, France, Sept. 2002.

[14] Cummings, E.B., Laser-induced thermal acoustics: simple accurate gas measurements, *Optics Letters* 19 (1994), No. 17, pp. 1361-1363.

[15] Cummings, E.B., Leyva, I.A., Hornung, H.G., Laser-induced thermal acoustics (LITA) signals from finite beams, *Applied Optics* 34 (1995), No. 18, pp. 3290–3302.

[16] Schlamp, S., *Laser-Induced Thermal Acoustic Velocimetry*, California Institute of Technology Pasadena, California, PhD thesis, 2000.

[17] Schlamp, S., Cummings, E.B., Hornung, H.G., Beam misalignments and fluid velocities in laser-induced thermal acoustics, *Applied Optics* 38 (1999), No. 27, pp. 5724–5733.

[18] Schlamp, S., Sobota, T.H., Measuring Concentrations with Laser-Induced Thermal Acoustics, *Proceedings in Applied Mathematics and Mechanics* 1 (2002), No. 1, pp. 260–261.

[19] Schlamp, S., Sobota, T.H., Measuring concentrations with laser-induced thermalization and electrostristion gratings, *Experiments in Fluids* 32 (2002), No. 6, pp. 683–688.

[20] Morley, C., Gaseq: A Chemical Equilibrium Program for Windows, `http://www.c.morley.dsl.pipex.com/`(accessed: 23.09.2010).

Appendix

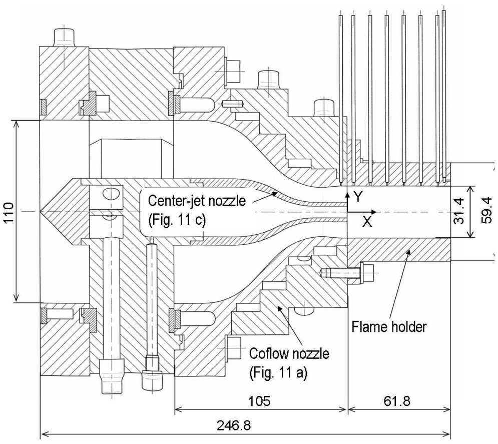

(a) Cross sectional view of the supersonic nozzle

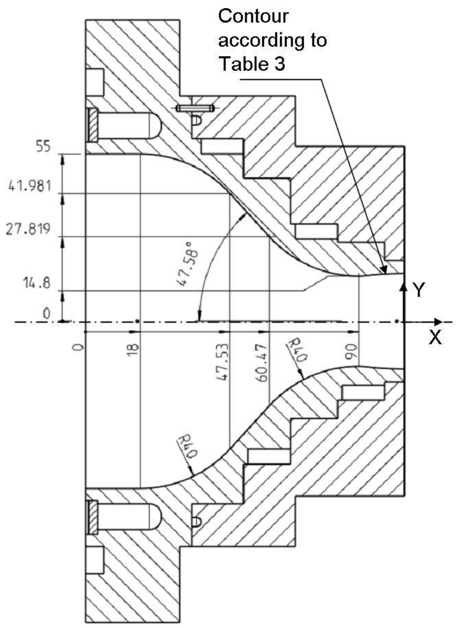

(b) Cross sectional view of the coflow nozzle

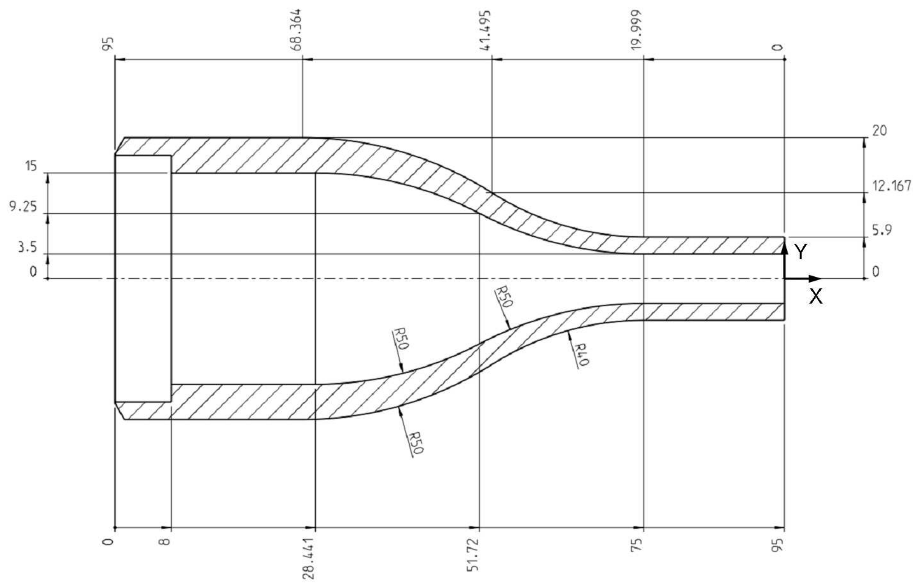

(c) Cross sectional view of the center-jet nozzle

Figure 11: Mechanical drawings of the supersonic nozzle

Table 3: Contour of the supersonic coflow nozzle

x [m]	y [m]
-1.5000000E-2	1.4800000E-2
-1.3834527E-2	1.4852831E-2
-1.2669055E-2	1.4965005E-2
-1.1503582E-2	1.5097446E-2
-1.0338110E-2	1.5220730E-2
-9.1726373E-3	1.5325085E-2
-8.0071647E-3	1.5412373E-2
-6.8416922E-3	1.5489167E-2
-5.6762196E-3	1.5556304E-2
-4.7088774E-3	1.5602533E-2
-3.9059834E-3	1.5632833E-2
-3.2395813E-3	1.5651891E-2
-2.6864676E-3	1.5664476E-2
-2.2273832E-3	1.5673229E-2
-1.8463432E-3	1.5679675E-2
-1.5300800E-3	1.5684552E-2
-1.2675815E-3	1.5688289E-2
-1.0497078E-3	1.5691282E-2
-8.6887256E-4	1.5693502E-2
-7.1877934E-4	1.5695163E-2
-5.9420197E-4	1.5696542E-2
-4.9080275E-4	1.5697688E-2
-4.0498140E-4	1.5698128E-2
-3.3374968E-4	1.5698458E-2
-2.7462736E-4	1.5698731E-2
-2.2555582E-4	1.5698958E-2
-1.8482645E-4	1.5699146E-2
-1.5102107E-4	1.5699302E-2
-1.2296261E-4	1.5699432E-2
-9.9674084E-5	1.5699540E-2
-8.0344608E-5	1.5699629E-2
-6.4301143E-5	1.5699703E-2
-5.0985067E-5	1.5699765E-2
-3.9932724E-5	1.5699816E-2
-3.0759279E-5	1.5699858E-2
-2.3145320E-5	1.5699893E-2
-1.6825734E-5	1.5699923E-2
-1.1580477E-5	1.5699947E-2
-7.2269144E-6	1.5699967E-2
-3.6134572E-6	1.5699984E-2
0.0000000E+0	1.5700000E-2